Physical Review Special Topics - Accelerators and Beams - Special Issue

21st ICFA Beam Dynamics Workshop on Laser-Beam Interactions

Thomson scattering sources of fs X-rays based on laser wakefield accelerators

E. Esarey, P. Catravas and W.P. Leemans

Center for Beam Physics, Accelerator and Fusion Research Division

Ernest Orlando Lawrence Berkeley National Laboratory

University of California, Berkeley CA 94720

Abstract

The production of ultrashort (fs) X-ray pulses through Thomson scattering of high power laser pulses off relativistic electron bunches generated by plasma-based accelerators is discussed. The electron bunches are produced with either a self-modulated laser wakefield accelerator (SM-LWFA) or through a standard laser wakefield accelerator (LWFA) with optical injection. For a SM-LWFA, the electron bunch has a high charge with a broad energy distribution, resulting in X-ray pulse with high flux with a broadband spectrum. For a LWFA with optical injection, the electron bunch can be ultrashort (fs) with a narrow energy distribution, resulting in an ultrashort X-ray pulse with a nearly monochromatic spectrum. Examples are given for sources of 3-100 fs X-ray pulses and the expected flux and brightness of these sources are calculated and compared.

I. INTRODUCTION

One approach to the generation of ultra-short X-ray pulses [1] is laser-based Thomson scattering (TS), where by an intense laser pulse is scattered off a relativistic electron beam [2]- [16]. The first demonstration of the generation of sub-picosecond duration X-ray pulses using 90° TS was performed at the Beam Test Facility of the Advanced Light Source at Lawrence Berkeley National Laboratory (LBNL) [6]- [8]. In these experiments, an X-ray pulse duration of 300 fs (FWHM) was measured, as determined by the convolution between the laser pulse duration (100 fs) and the crossing time of the laser across the tightly focused electron beam (200 - 250 fs). The number of X-rays and the peak brightness of the 90° TS source experiments at LBNL were limited, in part, by (i) the fact that the laser pulse only interacted with about a 100 fs long electron beam slice (or 0.3% of all the available electrons), (ii) the relatively high transverse emittance of the electron beam and (iii) the low peak power of the laser. To increase the photon yield and brightness of a TS source, high quality ultra-short electron bunches are needed in conjunction with a high-power laser system.

In this paper, TS sources are discussed that use ultra-short electron bunches produced with laser wakefield accelerators (LWFAs) [17]. The characteristic scale length of the accelerating field in a plasma-based accelerator is the plasma wavelength,

$$\lambda_p[\mu\mathrm{m}] \simeq 3.3 \times 10^{10} n_p^{-1/2}[\mathrm{cm}^{-3}], \tag{1}$$

where n_p is the plasma density. For LWFAs, the plasma density is in the range $n_p = 10^{18} - 10^{20}$ cm^{-3}, which indicates that the plasma wavelength is very short $\lambda_p \simeq 3 - 30$ μm or $\tau_p = \lambda_p/c \simeq 10 - 100$ fs. In a standard LWFA, an intense laser pulse of length $L_L \sim \lambda_p$ is used to impulsively drive a large amplitude plasma wave (wakefield) with phase velocity near c. Short electron bunches of length $L_b < \lambda_p$ can be injected into the wake for acceleration to high energy. In a standard LWFA that produces a high quality electron bunch (such as in the colliding pulse injector discussed below), the electron bunch duration is ultra-short,

$\tau_b \ll \tau_p$. Hence, a LWFA in principle can generate electron bunches of fs duration. In this case, a TS source can utilize a 180° (backscattering) interaction geometry to produce fs X-ray pulses while producing high X-ray yields (in comparison to 90° scattering), since in the backscatter configuration the X-ray pulse duration is approximately equal to the electron bunch duration.

Most LWFA experiments performed to date have operated in the self-modulated laser wakefield accelerator (SM-LWFA) regime. In the SM-LWFA [18]- [20], the plasma density is sufficiently high (e.g., $n_p \sim 10^{20}$ cm^{-3}) such that (i) the laser pulse extends over several plasma wavelengths, $L_L > \lambda_p$, and (ii) the laser power P_L exceeds the critical power [21] for relativistic self-focusing $P_c[\mathrm{GW}] \simeq 17(\lambda_p/\lambda_L)^2$, i.e., $P_L > P_c$, where λ_L is the laser wavelength. Once these conditions are satisfied, the laser pulse is violently unstable, which leads to a strong modulation of the laser pulse with period λ_p and the generation of an extremely large plasma wave. In fact, the wakefield becomes sufficiently large so as to self-trap a fraction of the background plasma electrons and accelerate them to high energy. The duration of the electron bunch is initially on the order of the laser pulse duration. Energies up to 100 MeV have been demonstrated in several experiments [22]- [30]. However, the energy spread is large (100%), since electrons originate from self-trapping of the background plasma.

To achieve a high quality accelerated electron bunch, the standard LWFA can be used in conjunction with a method for injecting short bunches ($L_b < \lambda_p$) into the wakefield. The production of electron bunches with low momentum spread and good pulse-to-pulse energy stability requires fs electron bunches to be injected with fs synchronization with respect to the plasma wake. Although conventional electron sources (photocathode or thermionic RF guns) have achieved sub-picosecond electron bunches, the requirements for injection into plasma-based accelerators are presently beyond the performance of these conventional electron sources. Novel schemes which rely on laser triggered injection of plasma electrons into a plasma wake have been proposed to generate the required fs electron bunches [31]- [35]. In laser injection schemes, ultra-short laser pulses are used to dephase background

plasma electrons (which are undergoing fluid oscillations in the wake of a standard LWFA), such that they become trapped and accelerated in the wakefield.

One laser injection method that has been proposed is the colliding pulse injector [33]- [35]. Three laser pulses are used: an intense pump pulse (denoted by subscript 1) for plasma wake generation, a forward going injection pulse (subscript 2), and a backward going injection pulse (subscript 3). The frequency, wavenumber, and normalized intensity are denoted by ω_i, k_i, and a_i $(i = 1, 2, 3)$. Here $a = eA/mc^2$ is the normalized vector potential of the laser pulse, often referred to as the laser strength parameter, which is related to the laser pulse intensity I_L and wavelength λ_L by

$$a^2 \simeq 7.3 \times 10^{-19} \lambda_L^2[\mu\mathrm{m}] I_L[\mathrm{W/cm}^2]. \tag{2}$$

assuming linear polarization. The pump pulse ($a_1^2 \sim 1$) is used to generate the wake via the standard LWFA mechanism. When the two injection pulses ($a_2^2 \sim a_3^2 \ll a_1^2$) collide some distance behind the pump pulse, they generate a slow ponderomotive beat wave with a phase velocity $v_{pb} \simeq \Delta\omega/2k_1 \ll c$, where $\Delta\omega = \omega_2 - \omega_3$ and $\Delta\omega^2 \ll \omega_1^2$. During the time in which the two injection pulses overlap, a two-stage acceleration process can occur, i.e., the slow beat wave injects plasma electrons into the fast wakefield for acceleration to high energies. The colliding pulse scheme has the ability to produce fs electron bunches with low fractional energy spreads using relatively low injection laser pulse intensities compared to the pump laser pulse. Injection and acceleration can occur at low densities ($\lambda_p/\lambda_1 \sim 100$), thus allowing for high single-stage energy gains. Furthermore, the colliding pulse concept offers detailed control of the injection process: the injection phase can be controlled via the position of the forward injection pulse, the beat phase velocity via $\Delta\omega$, the injection energy via the pulse amplitudes, and the injection time (number of trapped electrons) via the backward pulse duration. Estimates indicate that space charge effects can be neglected while the bunch remains inside the plasma [34] and can be minimized for sufficiently high energy electron beams [36].

In the following, two designs of novel ultra-short X-ray TS sources are discussed (one

based on a SM-LWFA, the other on a colliding pulse LWFA). In Sec. 2, analytic expressions for TS including broadening from an arbitrary energy distribution are presented. These expressions are valid when the number of laser periods in the interaction region is large and provide a new and efficient way to evaluate the broadened spectral flux density for the wide range of possible energy distributions which LWFAs can produce. The limiting case of a narrow Gaussian distribution is shown to agree with standard formulae, and the analysis is applied in the case of 100% energy spread, where standard formulae do not apply. In Sec. 3, TS designs using electron bunches produced via the SM-LWFA and a standard LWFA with optical injection are compared. The SM-LWFA yields large amounts of charge having large energy spread due to the uncontrolled trapping, and can provide X-ray flux over a large BW in a < 100 fs pulse. The colliding pulse all-optical injector [33]- [35], which utilizes optical methods for triggering the trapping of electrons, holds the promise to produce low emittance electron bunches with low energy spread, which can be used to generate high brightness X-ray pulses with a few fs pulse length.

II. PROPERTIES OF THOMSON SCATTERED X-RAYS

Thomson scattering of an intense laser beam from an electron beam is capable of producing directed, bright, short pulses of tunable X-rays, both as a radiation source as well as a means for diagnosing electron beams [8]. Effectively, the laser field acts as an electromagnetic undulator for the electron beam. Since the undulator period is determined by the laser wavelength, ultra-short wavelength radiation (X-rays or γ-rays) can be generated using electron beams of modest energies.

The X-ray wavelength, λ_x, of the radiation emitted from a single electron with relativistic factor γ is given by

$$\lambda_x = \frac{\lambda_L}{2n\gamma^2}\frac{(1+\gamma^2\theta^2+a^2/2)}{(1-\cos\psi)}, \tag{3}$$

assuming $\gamma^2 \gg (1+a^2/2)$, $\theta^2 \ll 1$, and linear polarization, where n is the harmonic number, ψ is the angle of interaction between the laser and the electron (e.g., $\psi = 180^\circ$ for head-

on scattering) and θ is the observation angle (relative to the initial electron trajectory). In the low intensity limit $a^2 \ll 1$, radiation is scattered only at the fundamental $n = 1$. In the nonlinear limit $a^2 \gg 1$, numerous harmonics are generated [3,4]. This results in a near continuum of scattered radiation with harmonics extending out to a critical harmonic number (e.g., $n_{cr} = 3a^3/4$ for $\psi = 180°$), beyond which the intensity of the scattered radiation rapidly decreases [3,4]. Note that here, because the laser photon energy in the electron beam rest frame ($\gamma\hbar\omega_L$) is much less than the electron rest energy (mc^2), Compton recoil can indeed be neglected. Also, for relativistic electron beams, the X-ray flux is strongly peaked in the forward direction with a radiation cone opening angle of $1/\gamma$.

In the limit $K_L^2 \ll 1$, the number of X-rays scatter per electron, at all angles and frequencies, is

$$N_{xs} = (\pi/3)\alpha_f a^2 N_L^*, \tag{4}$$

where N_L^* is the effective number of laser periods with which the electron interacts and $\alpha_f = 1/137$ is the fine structure constant.

A. Single electron spectrum

The general form of $d^2I/d\omega d\Omega$ (the energy radiated by a single electron per unit frequency, $d\omega$, per unit solid angle, $d\Omega$) is derived by integrating the Liénard-Wiechert potentials over the electron motion. For a linearly polarized plane wave laser pulse with a constant amplitude a_0 and length L propagating in along the $-z$ axis, and interacting with an electron with a relativistic factor $\gamma = (1-\beta^2)^{-1/2}$ propagating along the $+z$ axis, the spectral energy density is given by [3]

$$\frac{d^2I}{d\omega d\Omega} = \sum_{n=1}^{\infty} \frac{e^2k^2}{4\pi^2 c} \left(\frac{\sin \bar{k}L/2}{\bar{k}}\right)^2 \tag{5}$$

$$\cdot \left[C_x^2(1 - \sin^2\theta\cos^2\phi) + C_z^2 \sin^2\theta - C_x C_z \sin 2\theta \cos\phi\right], \tag{6}$$

where

$$C_x = \sum_{m=-\infty}^{\infty} (-1)^m k_0 r_1 J_m(\alpha_z) \left[J_{n-2m-1}(\alpha_x) + J_{n-2m+1}(\alpha_x) \right], \tag{7}$$

$$C_z = \sum_{m=-\infty}^{\infty} (-1)^m 2 J_m(\alpha_z) \{ \beta_1 J_{n-2m}(\alpha_x) \tag{8}$$

$$+ k_0 z_1 \left[J_{n-2m-2}(\alpha_x) + J_{n-2m+2}(\alpha_x) \right] \}, \tag{9}$$

and $J_{m,n}$ are Bessel functions with arguments

$$\alpha_z \simeq \frac{n a_0^2 (1+\cos\theta)}{8 h_0^2 \left[1 - \beta_1 (1+\cos\theta)\right]}, \tag{10}$$

$$\alpha_x \simeq \frac{n a_0 \sin\theta \cos\phi}{h_0 \left[1 - \beta_1 (1+\cos\theta)\right]}. \tag{11}$$

Here, $\omega = ck$ is the radiated frequency, $\omega_0 = ck_0$ is the laser frequency, $\bar{k} = k\left[1 - \beta_1(1+\cos\theta)\right] - nk_0$, $\beta_1 = (1/2)\left(1 - 1/M_0\right)$, $h_0 = \gamma(1+\beta)$, $M_0 = h_0^2/(1 + a_0^2/2)$, $r_1 = a_0/h_0 k_0$, and $z_1 = -a_0^2/8h_0^2 k_0$. The approximation $k \simeq k_r$ was made in the Bessel function arguments, α_x and α_z, where k_r is the resonant frequency defined by $\bar{k} = 0$,

$$k_r = \frac{n k_0}{\left[1 - \beta_1 (1+\cos\theta)\right]}, \tag{12}$$

and n is the harmonic number. In the limit $\theta^2 \ll 1$, this reduces to

$$k_r \simeq \frac{n\gamma^2 (1+\beta)^2 k_0}{\left[1 + a_0^2/2 + \gamma^2 (1+\beta)^2 \theta^2/4\right]}. \tag{13}$$

Throughout the following, the limit of low laser intensity will be considered, $a_0^2 \ll 1$. In this limit, energy is radiated primarily in only the $n = 1$ fundamental mode. Higher harmonic radiation becomes significant when a_0 approaches or exceeds unity [3]. In the limit $a_0^2 \ll 1$, $C_x \simeq k_0 r_1$ and $C_z \simeq \beta_1 \alpha_x$. Furthermore, for highly relativistic electrons, $\gamma^2 \gg 1$, the radiation is confined to narrow cone angles $\theta^2 \sim 1/\gamma^2 \ll 1$. Hence, in the limits $a_0^2 \ll 1$, $\gamma^2 \gg 1$, and $\theta^2 \ll 1$, the spectral energy density of the radiation is given by

$$\frac{d^2 I}{d\omega d\Omega} \simeq r_e m_e c \frac{\gamma^2 N_0^2 a_0^2}{(1+\gamma^2\theta^2)^2} \left[1 - \frac{4\gamma^2\theta^2 \cos^2\phi}{(1+\gamma^2\theta^2)^2} \right] R(\omega, \omega_0), \tag{14}$$

where $r_e = e^2/m_e c^2$ is the classical electron radius and $N_0 = 2\pi L/k_0$ is the number of periods in the laser pulse.

The resonance function, $R(\omega, \omega_0)$, determines many of the defining characteristics of Thomson scattered radiation:

$$R(\omega, \omega_0) = \left(\frac{\sin \bar{k} L/2}{\bar{k} L/2} \right)^2. \tag{15}$$

For $N_0 \gg 1$, the resonance function $R(\omega, \omega_0)$ is sharply peaked about the resonant frequency defined by $\bar{k} = k(1 + \gamma^2\theta^2)/(4\gamma^2) - k_0 = 0$, i.e., $\omega_r = 4\gamma^2\omega_0/(1 + \gamma^2\theta^2)$. Furthermore, the frequency width of the resonance function is given by $\Delta\omega_r = \int d\delta\omega R = \omega_r/N_0$, where $\delta\omega = \omega - \omega_r$. Of particular interest is the behavior for a large number of periods, N_0. In the limit $N_0 \to \infty$, $R \to \Delta\omega_r \delta(\omega - \omega_r) = \Delta\gamma_r \delta(\gamma - \gamma_r)$, where $\Delta\gamma_r = 2\gamma_r^3\omega_0/N_0\omega$. Here, γ_r is the resonant electron energy defined by $\bar{k} = 0$, i.e., $\gamma_r^2 \simeq \omega/(4\omega_0 - \omega\theta^2)$.

Of interested is the radiation collected by an axisymmetric detector placed along the axis some distance for the interaction point. In this case, Eq. (14) can be averaged over the azimuthal angle ϕ,

$$\frac{d^2 I}{d\omega d\Omega} \simeq r_e m_e c \gamma^2 N_0^2 a_0^2 \left[\frac{(1 + \gamma^4\theta^4)}{(1 + \gamma^2\theta^2)^4} \right] R(\omega, \omega_0). \tag{16}$$

B. Spectrum for arbitrary energy distribution

In general, the computation of spectral flux density from an electron bunch, including realistic spreads in beam parameters, is performed through convolution of the electron distribution with the single electron spectral flux density. For a normalized electron distribution function, $f(\gamma, \theta_e)$, the resulting spectral flux density of the TS radiation from an electron beam is given by

$$\frac{d^2 I_T}{d\omega d\Omega}(\theta, \omega) = \int d\theta_e d\gamma f(\theta_e, \gamma) \frac{d^2 I}{d\omega d\Omega}(\theta - \theta_e, \gamma, \omega), \tag{17}$$

where θ_e is the angle of the electron trajectory with respect to the longitudinal axis ($\theta_e^2 \ll 1$ is assumed). Here, the transverse dimensions of the electron bunch at the interaction point are assumed to be small compared to cone angle of the TS radiation at the point of

observation. In this case, integration over the transverse dimensions of the electron bunch can be neglected, as is done in the above expression.

The electron beams generated by different LWFA designs under current development exhibit strongly contrasting characteristics. When the electron energy distribution is narrow, standard formulae [2]- [8], [16] can be used to evaluate the contribution of energy spread to figures of merit such as the on-axis flux and brightness. Such is the case for the colliding pulse optical injection scheme [33]- [34] in the standard LWFA. However, when the energy distribution is broad, such as for the SM-LWFA, the standard formulae cannot be applied. They become inapplicable because the on-axis frequency, $4\gamma^2\omega_0$, ($a_0^2 \ll 1, \theta = 0$) can change by up to three orders of magnitude across the energy distribution, accompanied by a factor of thirty change in the on-axis opening angle, $1/(\gamma\sqrt{N_0})$. When a_0^2 is not small compared with unity, the situation is even more complex, as there is substantial overlap between harmonics [3,4] radiated by the lower energy electrons of the distribution and radiation at the fundamental by higher energy electrons.

Computations which include arbitrary electron energy distributions can be simplified by noticing that a very large number of periods N_0 is available in the interaction region (up to 1000's), so that the intrinsic spectral line broadening at any fixed angle is essentially a delta function compared with the contribution from the electron energy distribution for realistic parameters. In this case, analytic expressions can be obtained for the spectral flux density which are valid for typical electron energy distributions.

C. Spectrum for the SM-LWFA bunch

To include the effect of energy spread, the spectral flux density is integrated over the electron energy spectrum, $f(\gamma)$,

$$\frac{d^2I_T}{d\omega d\Omega} \simeq \int d\gamma f(\gamma) \frac{d^2I}{d\omega d\Omega}. \tag{18}$$

Beam emittance is neglected since the angular width of the spectrum over the photon energies of interest is much broader than typical beam divergences. Assume $f(\gamma)$ is slowly varying

compared to $R(\omega, \omega_r)$ for fixed ω. Integrating over the delta function approximation for $R(\omega, \omega_r)$ in frequency (energy) yields the following analytic form for the energy integrated spectrum

$$\frac{d^2 I_T}{d\omega d\Omega} \simeq \frac{r_e mc}{16} N_0 a_0^2 \left(\frac{\omega}{\omega_0}\right)^{3/2} f\left(\gamma = (\omega/4\omega_0)^{1/2}\right), \tag{19}$$

where $\gamma\theta \simeq (\omega/4\omega_0)^{1/2}\theta \ll 1$ has been assumed. Integrating the above expression over frequency ω gives

$$\frac{dI_T}{d\Omega} \simeq 4 r_e mc N_0 a_0^2 \omega_0 \int d\gamma \gamma^4 f(\gamma). \tag{20}$$

Of particular interest is the photon flux and brightness of the TS radiation. Assuming that the collection angle, θ_d, is small ($\theta_d < (\Delta\omega/\omega)^{1/2}/\gamma < (1/N)^{1/2}/\gamma$) so that the intensity distribution is flat over the solid angle $\Delta\Omega_d = \pi\theta_d^2$, the number of photons intercepted in a small bandwidth, $\Delta\omega$, about ω and solid angle, $\Delta\Omega_d$, for an electron bunch with N_b electrons is

$$N_T = \frac{N_b}{\hbar}\frac{d^2 I_T}{d\omega d\Omega}\frac{\Delta\omega}{\omega}\pi\theta_d^2 \simeq \frac{\alpha_f}{16} N_b N_0 a_0^2 \left(\frac{\omega}{\omega_0}\right)^{3/2} f\left(\gamma = (\omega/4\omega_0)^{1/2}\right)\frac{\Delta\omega}{\omega}\pi\theta_d^2, \tag{21}$$

where α_f is the fine structure constant. The average flux in photons per second, F_{ave}, in the collection angle θ_d and with bandwidth $\Delta\omega$, is N_T multiplied by the repetition rate, f_{rep}, of the laser/electron beam, i.e., $F_{ave} = N_T f_{rep}$. The average source brightness (in photons/s/mm^2/mrad^2/0.1% BW) is given by

$$B_{ave} = \frac{F_{ave}}{(2\pi)^2 {r_b}^2 {\theta_d}^2} \simeq \frac{\alpha_f N_b N_0 a_0^2}{64\pi r_b^2}\left(\frac{\omega}{\omega_0}\right)^{3/2} f\left(\gamma = (\omega/4\omega_0)^{1/2}\right)\frac{\Delta\omega}{\omega}, \tag{22}$$

where r_b is the electron bunch radius. The peak flux and brightness are, respectively, $F_{pk} = F_{ave}/(\tau_x f_{rep})$ and $B_{pk} = B_{ave}/(\tau_x f_{rep})$, where τ_x is the X-ray pulse duration, which is assumed to be approximately equal to the electron bunch duration. Note that the region of validity of Eqs. (16)-(18) is for $(\omega/4\omega_0)^{1/2} \geq \gamma_{min}$, where γ_{min} is the minimum γ of the electrons in the distribution $f(\gamma)$.

D. Spectrum for narrow energy distribution

For an electron bunch with a narrow energy spread $\Delta\gamma/\gamma_0 \ll 1$ about a mean energy, γ_0, and for a narrow distribution in beam angle with spread $\Delta\theta = \epsilon_n/\gamma r_b \ll 1$, where ϵ_n is the normalized emittance and r_b the beam radius, estimates for flux and brightness have been derived [3], [30]. In particular, the total number of photons scattered per laser-electron bunch interaction into a small bandwidth, $\Delta\omega/\omega \ll 1$, is approximately

$$N_T = 2\pi\alpha_f N_0 a_0^2 \frac{\Delta\omega}{\omega} N_b G_{coll}, \tag{23}$$

assuming $a_0^2 \ll 1$, where N_b is the number of electrons per bunch interacting with the laser pulse. Here, G_{coll} is a factor determined by the collection angle, θ_d, of the X-ray optics, i.e., $G_{coll} = \theta_d^2/(\theta_d^2 + \theta_T^2)$ with

$$\theta_T{}^2 \simeq \left[(\Delta\omega/\omega)^2 + (\Delta\omega/\omega)_0{}^2 + (\Delta\omega/\omega)_\epsilon{}^2 + (\Delta\omega/\omega)_i{}^2\right]^{1/2}/\gamma^2, \tag{24}$$

where $(\Delta\omega/\omega)_0 = 1/N_0$, $(\Delta\omega/\omega)_\epsilon = \epsilon_n{}^2/r_b{}^2$ and $(\Delta\omega/\omega)_i = 2\Delta\gamma/\gamma$ represent the contributions to the bandwidth from the finite interaction length, the beam emittance and energy spread, respectively. The average flux is $F_{ave} = N_T f_{rep}$ and the average brightness is

$$B_{ave} = \frac{N_T f_{rep}}{(2\pi)^2 \sigma_r^2 \sigma_\theta^2}, \tag{25}$$

where $\sigma_r \simeq r_b$ and $\sigma_\theta \simeq \theta_T$ are the rms source size and opening angle of the radiation, respectively, and $r_b \simeq r_0$ has been assumed, where r_0 is the laser pulse radius.

III. EXAMPLES BASED ON LWFAS

Two examples of TS sources are given, one based on the SM-LWFA and the other based on a standard LWFA with colliding pulse injection. Both use a head-on interaction geometry. These examples are summarized in Table I.

Parameter	**Coll. Pulse**	**SM-LWFA**	**BTF** [6]- [8]
Laser wavelength λ_L [μm]	0.8	0.8	0.8
Laser pulse energy U_L [J]	0.5	0.6	0.04
Laser pulse duration (FWHM) τ_L [ps]	1	1.4	0.1
Electron beam energy γ	50	Exp. Distribn.	98
Number of electrons N_b	3×10^7	3×10^{10}	8×10^9
Electron bunch length (FWHM) τ_b [ps]	0.003	0.1	30
Electron spot size (FWHM) r_b [μm]	6	6	90
Normalized emittance ϵ_N [mm-mrad]	1	1	30
Bandwidth $\delta\omega/\omega$	10^{-3}	10^{-3}	10^{-3}
Collection angle [mrad]	1	3	1
Repetition rate [Hz]	10	10	2
Flux (ph/s/0.1%BW) in coll. angle	5×10^4	2×10^5	6×10^2
Ave. brightness (ph/s mm^{2}mrad^2 0.1%BW)	1.5×10^8	9×10^7	3×10^3
Peak brightness (ph/s mm^{2}mrad^2 0.1%BW)	5×10^{21}	10^{20}	10^{16}
Tot. no. photons/s (all freq., all angles)	2×10^8	3×10^{11}	2×10^7
X-ray pulse length [fs]	3	< 100	300
X-ray photon energy [keV]	12.4	Broadband, max at 2-3 keV	30

TABLE I. Comparison of Thomson scattering source designs using laser wakefield accelerators and experimental results with an RF accelerator.

A. Self-Modulated Laser Wakefield Accelerator

The SM-LWFA provides short (< 100 fs), high charge ($> 10^{10}$ electrons) bunches having a broad energy distribution. Thus TS using a SM-LWFA injector will be characterized by

high photon flux with broad bandwidth. Bunch lengthening due to space charge effects [36] can be avoided by minimizing the propagation distance of the electron bunch before the TS interaction, thus keeping the electron bunch length as close as possible to the laser pulse length. Shorter drive pulse lengths combined with higher plasma densities can lead to shorter electron bunch lengths and higher X-ray brightness. That is, decreasing the laser pulse length $L = c\tau_L$ requires increasing plasma density to satisfy $L > \lambda_p$, and the wake axial electric field scales roughly as $E_z \sim \sqrt{n_p}$, where n_p is the plasma density.

Uncontrolled trapping leads to an energy distribution of the form [24]- [30]

$$f(\gamma) = \gamma_{eff}^{-1} \exp\left[-(\gamma - \gamma_{min})/\gamma_{eff}\right], \tag{26}$$

for $\gamma \geq \gamma_{min}$, where γ_{min} is the minimum γ for the electrons in the distribution, γ_{eff} is constant (a measure of the effective temperature of the distribution), and the distribution is normalized such that integration over γ from γ_{min} to infinity is unity. For the LBNL SM-LWFA experimental results [30], $1/\gamma_{eff} \simeq 0.15$ and $\gamma_{min} \simeq 3$, i.e., $f(\gamma) \simeq 0.24\exp(-0.15\gamma)$ for $\gamma \geq 3$. The total charge was also at least 5 nC per bunch, or 3×10^{10} particles, and was generated with a driving pulse of 50 fs with $a_0 \sim 1$ at 10 Hz and a plasma density of a few 10^{19} cm^{-3}.

Using these electron beam parameters, the following TS source may be designed. A 600 mJ, 1.4 ps laser pulse with a wavelength of 800 nm and a rep rate of 10 Hz is focussed to a spot size of 6 microns. With a corresponding a_0 of 0.7, about 3×10^{11} photons per second are radiated in all frequencies and all angles. The average X-ray flux (photons/s/0.1% BW), for a collection angle of 3 mrad and 10 mrad, as well as the average brightness (photons/s/mm^{2}mrad^2/0.1% BW), calculated with Eq. (22), as a function of photon energy are shown in Fig. 1. The average brightness for these parameters peaks between 2 and 3 keV and has a total bandwidth of about 10 keV. As the result of the use of an ultrashort laser pulse, the peak brightness ($B_{pk} = B_{ave}/\tau_x f_{rep} \sim$ 3-4$\times 10^{19}$ photons/s/mm^{2}mrad^2/0.1% BW) is 12 orders of magnitude higher than the average brightness for these parameters. The parameters and X-ray characteristics are summarized in Table 1, column 2.

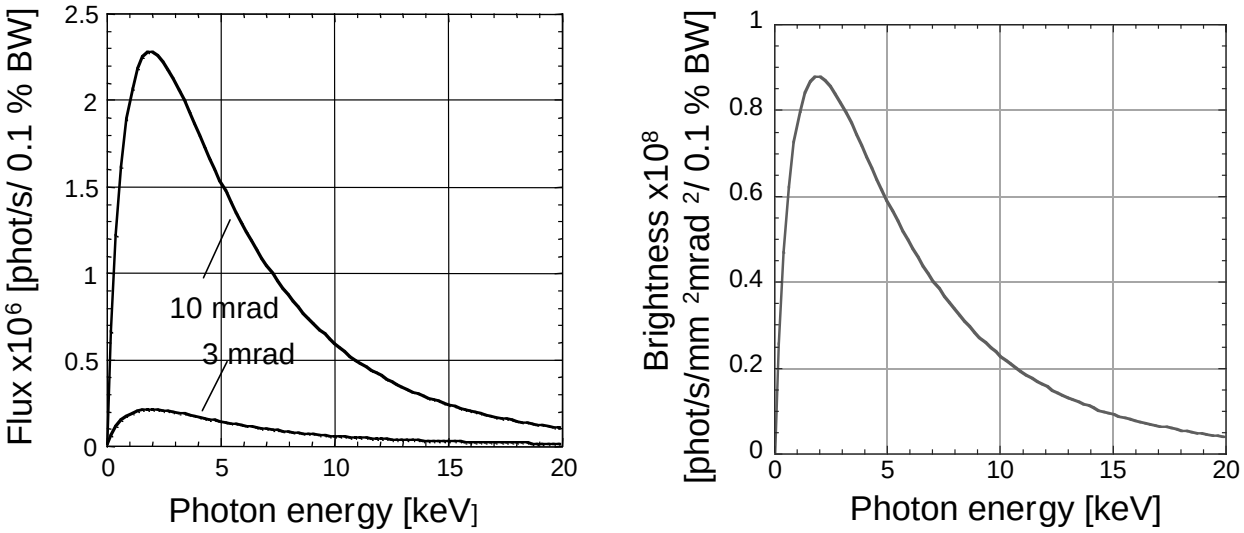

FIG. 1. The average flux (left) into 3 and 10 mrad collection angles and average brightness (right) for the SM-LWFA-based TS design (see Table 1, column 2 for parameters) shows the influence of the high charge per bunch (~ 5 nC) and broad energy distribution.

The average spectral flux density, $dF_{ave}/d\Omega$, over a range of 20 keV in photon energy and 50 mrad observation angle, in photons per second per 0.1% BW per solid angle, is shown in Fig. 2(d) for the SM-LWFA example. Here, $dF_{ave}/d\Omega = (N_b/\hbar)(d^2I_T/d\omega d\Omega)(\Delta\omega/\omega)f_{rep}$, where $d^2I_T/d\omega d\Omega$ is found by calculating Eq. (18) numerically. Figure 2(b) shows $dF_{ave}/d\Omega$ (blue curve) along the axis ($\theta = 0$) versus photon energy, as well as the electron distribution (red curve) versus γ. The higher the on-axis photon energy, corresponding to each slice in electron energy, the lower the amplitude. Beam emittance is about 1 π mm-mrad. Hence, for the corresponding photon divergences of $\sim$10 mrad, divergence broadening can be neglected for the bulk of the emissions (photon energies less than 15 keV).

B. Colliding Pulse All-Optical Injector

This section discusses the generation of near-monochromatic X-rays using TS off electron bunches produced with the colliding pulse laser-plasma electron source for generating truly femtosecond electron bunches [33]- [35]. The colliding pulse TS example is summarized in column 1 of Table 1. In this example, electron beam parameters based on the colliding pulse

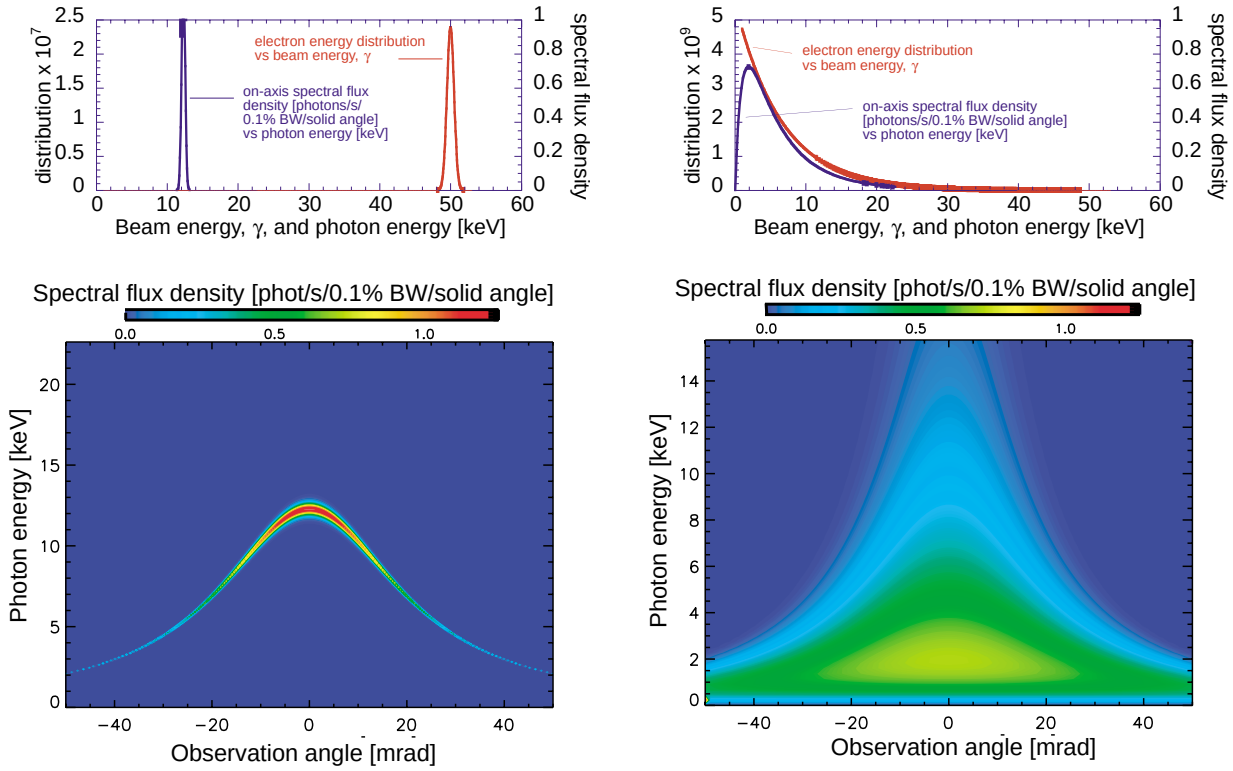

FIG. 2. Electron and X-ray properties for the colliding pulse LWFA, (a-upper left) and (c-lower left), and SM-LWFA, (b-upper right) and (d-lower right), examples for the parameters of Table 1. The electron energy (γ) distribution (red curve) and X-ray average spectral flux density (blue curve) along the axis ($\theta = 0$) are show in (a) and (b). The average spectral flux density, $dF_{ave}/d\Omega$ (10^{10} photons/s/0.1% BW/solid angle), as a function of photon energy (keV) and angle (θ) are shown in (c) and (d).

simulations discussed in Ref. [34] are used. An ultrashort (3 fs, FWHM) electron bunch (3×10^7 electrons), with a Gaussian energy distribution characterized by a mean energy of 25 MeV ($\gamma = 50$) and a fractional energy spread of 1% (RMS), a normalized transverse emittance of 1 mm-mrad, and a focal radius of 6 microns (FWHM) is assumed. A 0.8 micron laser with 500 mJ energy and 1 ps duration focussed to a 6 micron spot is also assumed. The design on-axis photon energy is 12.4 keV. For a rep rate of 10 Hz and a 1 mrad collection angle, the average brightness is about 10^8 photons/s/mm^{2}mrad^2/0.1% BW. Due to the low contributions of inhomogeneous broadening, the peak brightness of 5×10^{21} photons/s/mm^{2}mrad^2/0.1% BW is two orders of magnitude higher than for the SM-LWFA in spite of 3 orders of magnitude lower total flux into all angles and frequencies. This example indicates that this unique source, capable of producing truly femtosecond pulses, should have sufficient flux and brightness to perform pump-probe type experiments.

The average spectral flux density, $dF_{ave}/d\Omega$, versus photon energy and observation angle, in photons per second per 0.1% BW per solid angle, is shown in Fig. 2(c) for the colliding pulse LWFA example. Figure 2(a) shows $dF_{ave}/d\Omega$ (blue curve) along the axis ($\theta = 0$) versus photon energy, as well as the electron distribution (red curve) versus γ. The profile in Fig. 2(c) can be thought of as a composite slice of the SM-LWFA profile of Fig. 2(d). The energy distribution for the SM-LWFA is similar to a weighted sum of narrow energy slices, and the topography of the spectral flux density of the SM-LWFA arises from a sum of weighted contributions similar to that of Fig. 2(c), each having a different on-axis frequency. Note also that because N_0 is large, the spectral flux density contains a clear signature of the energy distribution in both designs and can be used as a diagnostic.

IV. CONCLUSION

Laser wakefield accelerators provide electron bunches suitable for the production of ultrashort, high brightness X-ray pulses through 180° Thomson scattering. To date the study of ultrafast processes has largely relied on femtosecond optical pulses from mode-locked lasers.

Since X-rays interact with core electronic levels and hence are effective structural probes, the availability of femtosecond X-ray pulses and the intrinsic synchronization between laser and X-ray pulses would make it possible to directly probe changes in atomic structure on ultrafast time scales.

The self-modulated laser wakefield accelerator provides high charge (5 nC) in bunches of less than 100 fs at 100% energy spread (the bulk of the distribution is at energies of a couple of MeV with a exponential tail extending out to tens of MeV). The TS spectrum and spatial profile is characteristically broad. Based on current measured values for such electron bunches, a design having $a_0 < 1$ which sets the bulk of the photon energies in the range of a few keV has been described. Peak brightnesses are predicted to exceed 10^{19} photons/s/mm^{2}mrad^2/0.1% BW.

The proposed colliding pulse optical injection scheme has the ability to produce electron bunches of a few fs, having low energy spread and emittance. While charge levels are lower than for the SM-LWFA, low energy spread and divergence enables an increase of two orders of magnitude in peak brightness.

Although summarizing source performance using a single number (e.g., peak brightness) can be useful for some applications, proper evaluation must be made based on the type of experiment and its requirements, as well as on the ease of implementation and available infrastructure. These laser-plasma electron beam sources offer some unique advantages: (1) TS based sources can produce tunable ultra-short X-ray pulses using relatively low energy electron beams. (2) The source parameters such as photon energy, brightness, and bandwidth, are controllable through electron beam and laser parameters. For example, rapid polarization and wavelength control is possible through the laser polarization and wavelength tuning, respectively. (3) The X-ray pulse length is controllable through the laser pulse length, electron bunch length, and interaction geometry. (4) These laser-plasma methods provide perfect synchronization between the laser pulse, electron bunch, and X-ray pulse.

In addition to TS as an X-ray source, TS has utility as a novel electron beam diagnostic

technique. The use of short-pulse TS at 90 degrees as a diagnostic for electron bunches with low energy spread has already been demonstrated by Leemans et al. [8]. In addition, TS can be a useful diagnostic for electron bunches with large energy spread. As is evident for Eqs. (19)-(22), a measurement of the spectrum, flux, or brightness as a function of ω is an indirect measurement of the electron energy spectrum $f(\gamma)$, e.g., $d^2I_T/d\omega d\Omega \sim \hat{\omega}^{3/2} f(\gamma = \hat{\omega}^{1/2})$, where $\hat{\omega} = \omega/4\omega_0$.

These laser-plasma sources of X-rays are of table-top size. The major equipment required for such a source is a high power, chirp-pulse amplification laser system, which is becoming commonplace [37]. However, for all laser-plasma sources, laser repetition rate and average power have been some of the main limitations. Future research into the development of high average power lasers, as well as optical storage cavities for ultra-short pulses, would have a tremendous impact on the scientific reach of these laser-plasma based sources.

V. ACKNOWLEDGMENTS

This work was supported by the Department of Energy under Contract No. DE-AC-03-76SF0098.

REFERENCES

[1] See, for example, Special Issue on New Ultrafast X-ray Sources and Their Applications, ed. by J.C. Gauthier, Les Comptes Rendus de l'Académie des Sciences, Série IV **1** (2000).

[2] P. Sprangle, A. Ting, E. Esarey and A. Fisher, J. Appl. Phys. **72**, 5032 (1992); P. Sprangle and E. Esarey, Phys. Fluids B **4**, 2241 (1992); E. Esarey, P. Sprangle, A. Ting and S.K. Ride, Nucl. Instr. Meth. A **331**, 545 (1993).

[3] E. Esarey, S.K. Ride and P. Sprangle, Phys. Rev. E **48**, 3003 (1993).

[4] S.K. Ride, E. Esarey and M. Baine, Phys. Rev. E **52**, 5425 (1995); E. Esarey, S.K. Ride, M. Baine, A. Ting and P. Sprangle, Nucl. Instr. Meth. A **375**, 545 (1996).

[5] K.J. Kim, S. Chattopadhyay and C.V. Shank, Nucl. Instr. & Meth. A **341**, 351 (1994).

[6] R.W. Schoenlein, W.P. Leemans, A.H. Chin, P. Volfbeyn, T.E. Glover, P. Balling, M. Zolotorev, K.J. Kim, S. Chattopadhyay and C.V. Shank, Science **274**, 236 (1996).

[7] W.P. Leemans, R.W. Schoenlein, P. Volfbeyn, A.H. Chin, T.E. Glover, P. Balling, M. Zolotorev, K.J. Kim, S. Chattopadhyay and C.V. Shank, Phys. Rev. Lett. **77**, 4182 (1996).

[8] W.P. Leemans, R.W. Schoenlein, P. Volfbeyn, A.H. Chin, T.E. Glover, P. Balling, M. Zolotorev, K.J. Kim, S. Chattopadhyay and C.V. Shank, IEEE J. Quantum Electron. **33**, 1925 (1997).

[9] A. Ting, R. Fischer, A. Fisher, K. Evans, R. Burris, J. Krall, E. Esarey and P. Sprangle, J. Appl. Phys. **78**, 575 (1995); A. Ting, R. Fischer, A. Fisher, C.I. Moore, B. Hafizi, R. Elton, K. Krushelnick, R. Burris, S. Jackel, K. Evans, J.N. Weaver, P. Sprangle, E. Esarey, M. Baine and S.K. Ride, Nucl. Instr. Meth. A **375**, 68 (1996).

[10] F. Glotin, J.-M. Ortega, R. Prazeres, G. Devanz and O. Marcouille, Phys. Rev. Lett.

77, 3130 (1996).

[11] F.E. Carroll, J.W. Waters, R.H. Traeger, M.H. Mendenhall, W.-W. Clark and C.A. Brau, SPIE Proceedings **3614**, 139, (1999).

[12] G. Krafft, Jefferson Laboratory, private communication (1999).

[13] M. Uesaka, H. Kotaki, K. Nakajima, H. Harano, K. Kinoshita, T. Watanabe, T. Ueda, K. Yoshii, M. Kando, H. Dewa, S. Kondo and F. Sakai, Nucl. Instr. Meth. A **455**, 90-8 (2000).

[14] S. Kashiwagi, M. Washio, T. Kobuki, R. Kuroda, I. Ben-Zvi, I. Pogorelsky, K. Kusche, J. Skaritka, V. Yakimenko, X.J. Wang, T. Hirose, K. Dobashi, T. Muto, J. Urakawa, T. Omori, T. Okugi, A. Tsunemi, Y. Liu, P. He, D. Cline and Z. Segalov, Nucl. Instr. Meth. A **455**, 36-40 (2000).

[15] I.V. Pogorelsky, I. Ben-Zvi, T. Hirose, S. Kashiwagi, V. Yakimenko, K. Kusche, P. Siddons, J. Skaritka, T. Kumita, A. Tsunemi, T. Omori, J. Urakawa, M. Washio, K. Yokoya, T. Okugi, Y. Liu, P. He and D. Cline, Phys. Rev. Spec. Topics Accel. Beams **3**(9), 090702 (2000).

[16] W.P. Leemans, S. Chattopadhyay, E. Esarey, A. Zholents, M. Zolotorev, A. Chin, R. Schoenlein, and C.V. Shank, Les Comptes Rendus de l'Académie des Sciences, Série IV **1**, 279 (2000).

[17] E. Esarey, P. Sprangle, J. Krall, and A. Ting, IEEE Trans. Plasma Sci. **PS-24**, 252 (1996).

[18] E. Esarey, J. Krall and P. Sprangle, Phys. Rev. Lett. **72**, 2887 (1994).

[19] W.B. Mori et al., Phys. Rev. Lett. **72**, 1482 (1994).

[20] N.E. Andreev et al., Physica Scripta **49**, 101 (1994).

[21] E. Esarey, P. Sprangle, J. Krall and A. Ting, J. Quant. Electron. **33**, 1879-1914 (1997).

[22] A. Modena, Z. Najmudin, A.E. Dangor, C.E. Clayton, K.A. Marsh, C. Joshi, V. Malka, C.B. Darrow, C. Danson, D. Neely, and F.N. Walsh, Nature **377**, 606 (1995).

[23] K. Nakajima, D. Fisher, T. Kawakubo, H. Nakanishi, A. Ogata, Y. Kato, Y. Kitagawa, R. Kodama, K. Mima, H. Shiraga, K. Suzuki, K. Yamakawa, T. Zhang, Y. Sakawa, T. Shoji, Y. Nishida, N. Yugami, M. Downer, and T. Tajima, Phys. Rev. Lett. **74**, 4428 (1995).

[24] D. Umstadter, S.-Y. Chen, A. Maksimchuk, G. Mourou, and R. Wagner, Science **273**, 472 (1996); R. Wagner, S.Y. Chen, A. Maksimchuk, and D. Umstadter, Phys.Rev.Lett., **78**, 3125 (1997).

[25] A. Ting, C.I. Moore, K. Krushelnick, C. Manka, E. Esarey, P. Sprangle, R. Hubbard, H.R. Burris, and M. Baine, Phys. Plasmas **4**, 1889 (1997); C. Moore, A. Ting, K. Krushelnick, E. Esarey, R.F. Hubbard, H.R. Burris, C. Manka, and P. Sprangle, Phys. Rev. Lett. **79**, 3909 (1997).

[26] D. Gordon, K.C. Tzeng, C.E. Clayton, A.E. Dangor, V. Malka, K.A. Marsh, A. Modena, W.B. Mori, P. Muggli, Z. Najmudin, D. Neely, C. Danson, and C. Joshi, Phys. Rev. Lett. **80**, 2133 (1998).

[27] F. Amiranoff, S. Baton, D. Bernard, B. Cros, D. Descamps, L.F. Dorchies, F. Jacquet, V. Malka, J.R. Marques, G. Matthieussent, P. Mine, A. Modena, P. Mora, J. Morillo and Z. Najmudin, Phys. Rev. Lett. **81**, 995 (1998).

[28] F. Dorchies, F. Amiranoff, V. Malka, J.R. Marques, A. Modena, B. Cros, G. Matthussent, P. Mora, A. Solodov, J. Morillo and Z. Najmudin, Phys. Plasmas **6**, 2903 (1999).

[29] M.I.K. Santala, Z. Najmudin, E.L. Clark, M. Tatarakis, K. Krushelnick, A.E. Dangor, V. Malka, J. Faure, R. Allott, and R.J. Clarke, Phys. Rev. Lett. **86**, 1227 (2001).

[30] W.P. Leemans, D. Rodgers, P.E. Catravas, C.G.R. Geddes, G. Fubiani, E. Esarey, B.A.

Shadwick, R. Donahue, and A. Smith, Phys. Plasmas **8**, 2510 (2001).

[31] D. Umstadter, J.K. Kim, and E. Dodd, Phys. Rev. Lett. **76**, 2073 (1996).

[32] R. G. Hemker, K.-C. Tzeng, W.B. Mori, C.E. Clayton, and T. Katsouleas, Phys. Rev. E **57**, 5920 (1998).

[33] E. Esarey, R.F. Hubbard, W.P. Leemans, A. Ting, and P. Sprangle, Phys. Rev. Lett. **79**, 2682 (1997).

[34] C.B. Schroeder, P.B. Lee, J.S. Wurtele, E. Esarey, and W.P. Leemans, Phys. Rev. E **59**, 6037 (1999).

[35] E. Esarey, C.B. Schroeder, W.P. Leemans, and B. Hafizi, Phys. Plasmas **6**, 2262 (1999).

[36] G. Fubiani, W. Leemans and E. Esarey, in *Advanced Accelerator Concepts*, edited by P. Colestock and S. Kelly, AIP Conf. Proc. **569** (Amer. Inst. Phys., NY, 2001), pp. 423-435.

[37] G.A. Mourou, C.P.J. Barty and M.D. Perry, Physics Today **51**, 22-28, (1998).